Appl. Math. Mech. -Engl. Ed., **32**(8), 981–996 (2011)
DOI 10.1007/s10483-011-1474-7

Applied Mathematics and Mechanics (English Edition)

Diagonal form fast multipole boundary element method for 2D acoustic problems based on Burton-Miller boundary integral equation formulation and its applications*

Hai-jun WU (吴海军)[1], Wei-kang JIANG (蒋伟康)[1], Y. J. LIU[2]

(1. State Key Laboratory of Machinery System and Vibration, Shanghai Jiao Tong University, Shanghai 200240, P. R. China;
2. Mechanical Engineering, University of Cincinnati, Cincinnati, Ohio 45221-0072, USA)

Abstract This paper describes formulation and implementation of the fast multipole boundary element method (FMBEM) for 2D acoustic problems. The kernel function expansion theory is summarized, and four building blocks of the FMBEM are described in details. They are moment calculation, moment to moment translation, moment to local translation, and local to local translation. A data structure for the quad-tree construction is proposed which can facilitate implementation. An analytical moment expression is derived, which is more accurate, stable, and efficient than direct numerical computation. Numerical examples are presented to demonstrate the accuracy and efficiency of the FMBEM, and radiation of a 2D vibration rail mode is simulated using the FMBEM.

Key words 2D acoustic wave problem, Helmholtz equation, fast multipole method, boundary element method

Chinese Library Classification O348.8
2010 Mathematics Subject Classification 74S15

1 Introduction

The boundary element method (BEM), also referred to as the boundary integral equation (BIE) method, has been used to solve acoustic problems for many years[1–4]. The BEM discretizes the boundary only instead of the domain, which takes less CPU time due to the one-dimension reduction in mesh generations. However, the BEM has some drawbacks. The most troublesome one is that the BEM leads to systems of equations with dense and non-symmetrical coefficient matrices. Therefore, the size of the memory for storing coefficient matrix generated by BEM is $O(N^2)$, with N being the number of degrees of freedom. Solving the BEM systems of equations directly, such as by Gauss elimination method, will need $O(N^3)$ arithmetic

* Received Jun. 10, 2010 / Revised May 10, 2011
Project supported by the National Natural Science Foundation of China (No. 11074170) and the State Key Laboratory Foundation of Shanghai Jiao Tong University (No. MSVMS201105)
Corresponding author Wei-kang JIANG, Professor, Ph. D., E-mail: wkjiang@sjtu.edu.cn

operations. Thus, memory cost and solution time have been the limiting factors for solving large-scale acoustic problems by the BEM.

To overcome the drawback in numerical computation in the BEM, much work has been devoted to finding efficient methods to solve the BEM equations with less memory and CPU time. In the mid of 1980s, the fast multipole method (FMM) was innovated by Rokhlin and Greengard[5–7]. FMM can improve solution of the BEM systems of equations dramatically and decrease memory and CPU time from $O(N^2)$ to $O(N)$. The key idea behind the FMM is the multipole expansion of the kernel in which the connection between the field point and the source point is separated.

The FMM was later extended to 2D Helmholtz equation. There are some papers dealing with the FMM for 2D acoustic problems[8–11]. Rokhlin[8] discussed an algorithm for the rapid solution of boundary value problems for 2D Helmholtz equation based on iterative computation. Amini and Profit[9] described a one-level diagonal form FMM for 2D scattering theory. Amini and Profit[10] also studied the multi-level fast multipole solution of Burton and Miller's hypersingular formulation for the Helmholtz equation in 2D scattering problem. Chen and Chen[11] employed the concept of the FMM to accelerate the construction of influence matrix in the dual boundary integral equation method for exterior acoustic problems. For 3D acoustic wave problems, Liu, Shen, and Bapat have done extensive research on the fast multipole BEM (FMBEM) for both full-space and half-space problems[12–14].

There are actually two forms of the FMM for Helmholtz equation in [8–14], one is based on convolution form and the other is based on diagonal form. Both of them fail in some way outside their preferred frequency regime. Using convolution form FMM at the high frequency problem results in algorithms whose CPU time requirements are $O(p^3)$ with p being the truncation number, while employing diagonal form FMM at the low frequency problem leads to numerical instability. A lot of work has been done to overcome this problem. Both the underlying theory and some of the practical aspects of implementation to allow for stability and high accuracy at all wavelengths of a simple version of the FMBEM for the Helmholtz equation in two dimensions are described in Ref. [15]. Wideband FMBEM by combining convolution and diagonal form are proposed[16–17]. Although wideband FMBEM is stable and efficient for any frequency which is greater than zero, there is still room for the improvement of diagonal FMBEM which can make the wideband FMBEM performance better in return.

Following Ref. [18], which is an in-depth introduction to the fast multipole BEM (FMBEM) for 2D potential problems, the basic theory and algorithm of the FMBEM for 2D acoustic wave problems are discussed in this paper. The kernel function expansion theory, data structure for programming and the four building blocks (moment calculation, moment to moment, moment to local expansion, and local expansion to local expansion) are described in details. An analytical moment expression is proposed.

This paper is organized as follows: In Section 2, we begin with a brief description of the boundary integral equation (BIE) formulation for 2D acoustic problems and the conventional BEM. In Section 3, the multipole expansion theory is described, which is the foundation of the FMBEM. In Section 4, we provide the formulations for the four essential building blocks: moment calculation (M), moment to moment translation (M2M), moment to local translation (M2L), and local to local translation (L2L). In Section 5, a data structure for the quad-tree construction which can facilitate the implementation is proposed. Analytical moment expression is derived which is accurate, stable and efficient. Some other remarks concerning program implementation are also described in this section. Numerical examples and an application are presented in Section 6 to demonstrate the efficiency and validity of the FMBEM. Finally, a summary is given in Section 7 to conclude this paper.

2 Boundary integral equation and conventional BEM

2.1 2D acoustic problem and its BIE formulation

Consider a 2D object with boundary Γ in an infinite acoustic medium of mean density ρ and speed of sound c as shown in Fig. 1. The governing differential equation for steady-state linear acoustics is the following well known Helmholtz equation:

$$\nabla^2\varphi + k^2\varphi = 0, \tag{1}$$

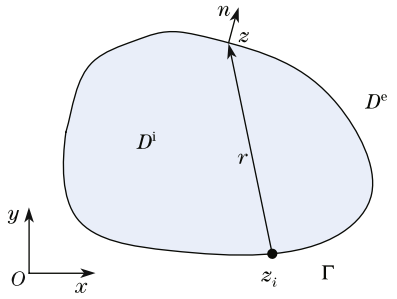

Fig. 1 2D exterior domain and its boundary

where φ is the sound pressure, and k is the wave number defined by $k = w/c$, in which w is the angular frequency. By using Green's second identity, (1) is reformulated into integral equation as follows[19]:

$$\varphi(z_i) = \int_\Gamma \Big(\frac{\partial G(z, z_i)}{\partial n(z)}\varphi(z) - G(z, z_i)q(z)\Big)\mathrm{d}\tau + \varphi^{\mathrm{I}}(z_i), \quad \forall z_i \in D, \tag{2}$$

where z_i is a field point and z is a source point on boundary Γ, $D = D^{\mathrm{e}} \cup D^{\mathrm{i}}$, $n(z)$ is the normal vector at point z (pointing into the exterior or interior domain for exterior and interior respectively). Also, φ^{I} is an incident wave and will not present for radiation problems, $q(z) = \frac{\partial\varphi(z)}{\partial n}$. In this paper, time convention adopted is $\mathrm{e}^{-\mathrm{i}wt}$, so the free space Green's function G for 2D problems is given by

$$G(z, z_i) = \frac{\mathrm{i}}{4}H_0^1(k\|\bar{z} - \bar{z}_i\|), \tag{3}$$

in which $\mathrm{i} = \sqrt{-1}$, $\bar{z} = [x\ y]$, and operator $\|\bar{z}\| = \sqrt{x^2 + y^2}$.

Letting point z_i approach the boundary leads to the following conventional boundary integral equation (CBIE):

$$c(z_i)\varphi(z_i) = \int_\Gamma \Big(\frac{\partial G(z, z_i)}{\partial n(z)}\varphi(z) - G(z, z_i)q(z)\Big)\mathrm{d}\tau + \varphi^{\mathrm{I}}(z_i), \quad \forall z_i \in \Gamma, \tag{4}$$

where constant $c(z_i) = 1/2$ if Γ is smooth around point z_i.

There is a defective concerning the CBIE for unique solution of exterior acoustic problem at the eigen-frequency associated with corresponding interior problem. To deal with the non-uniqueness difficulties, Burton and Miller[20] proposed a method by combining the CBIE and the normal derivative of the CBIE. Taking the derivative of integral representation equation (2)

with respect to the normal at the field point z_i and also letting point z_i approach the boundary lead the following hypersingular boundary integral equation (HBIE):

$$c(z_i)q(z_i)=\int_\Gamma\Big(\frac{\partial^2G(z,z_i)}{\partial n(z_i)\partial n(z)}\varphi(z)-\frac{\partial G(z,z_i)}{\partial n(z)}q(z)\Big)\mathrm{d}\tau+q^{\mathrm{I}}(z_i),\quad\forall z_i\in\Gamma. \tag{5}$$

For an exterior problem, (4) and (5) have a different set of fictitious frequencies at which a unique solution for the exterior problem cannot be obtained. However, (4) and (5) will always have only one solution in common. Given this fact, the following linear combination of (4) and (5) (CHBIE) should yield a unique solution for all frequencies:

$$\begin{aligned}&c(z_i)\varphi(z_i)-\varphi^{\mathrm{I}}(z_i)-\int_\Gamma\Big(\frac{\partial G(z,z_i)}{\partial n(z)}+\alpha\frac{\partial^2G(z,z_i)}{\partial n(z_i)\partial n(z)}\Big)\varphi(z)\mathrm{d}\tau\\&=\alpha q^{\mathrm{I}}(z_i)-\alpha c(z_i)q(z_i)-\int_\Gamma\Big(G(z,z_i)+\alpha\frac{\partial G(z,z_i)}{\partial n(z_i)}\Big)q(z)\mathrm{d}\tau,\end{aligned} \tag{6}$$

where α is a coupling constant that can be chosen as i/k[21]. This CHBIE formulation is referred to as the Burton-Miller formulation.

The main task of solving a 2D acoustic problem is to solve the boundary integral equation (6) together with impedance boundary condition. The general impedance boundary condition is

$$\mathrm{i}\rho w\widetilde{\varphi}(z)+\sigma\frac{\partial\widetilde{\varphi}(z)}{\partial n}\Big|_{z\in\Gamma}=0, \tag{7}$$

in which σ is the boundary impedance. The two extreme situations are Newman boundary condition corresponding to $\sigma=\infty$ and Dirichlet boundary condition corresponding to $\sigma=0$.

In the case of 2D exterior acoustic problem, (2) implicitly satisfies the 2D Sommerfeld radiation condition

$$\lim_{r\to\infty}r^{\frac{1}{2}}\Big(\frac{\partial}{\partial n}\varphi-\mathrm{i}k\varphi\Big)=0, \tag{8}$$

where $r=\|z\|$, $z\in D^{\mathrm{e}}$. This condition ensures that the solution of (6) is an outgoing wave[22].

2.2 Conventional BEM

(6) is usually solved by discretizing the equation and then applying numerical solutions. As an example of 2D discretization, for convenience, we use constant boundary elements, i.e., dividing the boundary Γ into N line segments and placing one node on each segment. After discretization, we obtain the following linear equations for node i ($i=1,2,\cdots,N$):

$$\sum_{j=1}^N\alpha_{ij}\varphi_j=\sum_{j=1}^N\beta_{ij}q_j+b^{\mathrm{I}}, \tag{9}$$

where b^{I} is from incident wave for scattering problem,

$$\alpha_{ij}=\int_{\Gamma_j}\Big(\frac{\partial G(z,z_i)}{\partial n(z)}+\alpha\frac{\partial^2G(z,z_i)}{\partial n(z_i)\partial n(z)}\Big)\mathrm{d}\tau-\frac{1}{2}\delta_{ij}, \tag{10}$$

$$\beta_{ij}=\int_{\Gamma_j}\Big(G(z,z_i)+\alpha\frac{\partial G(z,z_i)}{\partial n(z_i)}\Big)\mathrm{d}\tau+\frac{\alpha}{2}\delta_{ij}. \tag{11}$$

For $i \neq j$, regular integration methods such as Gauss integration can be used to calculate α_{ij} and β_{ij}. For $i = j$, $\frac{\partial G(z,z_j)}{\partial n_j}|_{z\in\Gamma_j} = 0$ holds for all elements, α_{ij} become hypersingular, and β_{ij} become singular, some special techniques should be used to compute them. Hadamard finite part integral is applied to compute hypersingular integral while the following integral[23] is used to calculate the singular integral:

$$\int_0^{\frac{l_j}{2}} G(z,z_i)\mathrm{d}\tau = \frac{\mathrm{i}l_j}{8}\Big(H_0^1\Big(\frac{kl_j}{2}\Big) + \frac{\pi}{2}\Big(S_0\Big(\frac{kl_j}{2}\Big)H_1^1\Big(\frac{kl_j}{2}\Big) - S_1\Big(\frac{kl_j}{2}\Big)H_0^1\Big(\frac{kl_j}{2}\Big)\Big)\Big), \tag{12}$$

where S_0 and S_1 are Struve function, and l_j is the length of element j.

By applying the N known boundary conditions, either φ or q at each element is known, and switching the columns in the two matrices in (9), a standard linear system of equations is formed as follows:

$$\begin{pmatrix} a_{11} & \cdots & a_{1N} \\ \vdots & & \vdots \\ a_{N1} & \cdots & a_{NN} \end{pmatrix} \begin{pmatrix} x_1 \\ \vdots \\ x_N \end{pmatrix} = \begin{pmatrix} b_1 \\ \vdots \\ b_N \end{pmatrix}, \quad \text{or} \quad Ax = b, \tag{13}$$

where A is the coefficient matrix which is full in general and non-symmetric, x is the unknown vector composing of unknown variables φ and q, and b is the known right-hand side vector computed from the known boundary values.

In conventional BEM, obviously the construction of matrix A requires $O(N^2)$ arithmetic operations, and the size of the required memory for storing A is also $O(N^2)$ since A is in general non-symmetric and dense. Solving the system in (13) by iterative solvers such as the generalized minimum residue (GMRES) method[24] or the conjugate gradient squared (CGS)[25] needs $O(N^2)$ operations to perform matrix-vector multiplication at each iteration in the conventional way. It is even worse to solve (13) by direct solvers such as Gauss elimination, which requires $O(N^3)$ arithmetic operations. That makes the conventional BEM approach unsuitable for solving large-scale problems.

3 Multipole expansion of kernel

The fast multipole method can be employed to accelerate the matrix-vector multiplication for solving (13) by using iterative solvers. The key idea behind the FMM is multipole expansion of the kernels in which the connection between the collocation point and the source point is separated, and then the elements-to-element interactions are replaced by cell-to-cell interactions.

The expansion results of the kernel H_0^1 are scattered in the references[10,26] and summarized herein for completeness. Based on Graf addition and integral identity for the first kind Bessel function of integer order, the free space Green's function of 2D acoustic problems can be expressed as the multipole expansion in the following, if $\|(\bar{z}_i - \bar{z}_L) - (\bar{z} - \bar{z}_c)\| < \|\bar{z}_c - \bar{z}_L\|$,

$$G(\bar{z},\bar{z}_i) \approx \frac{\mathrm{i}}{4L} f_k(z_i,z_L)T_k(z_L,z_c)g_k(z_c,z), \tag{14}$$

where $f_k = (f_k^0 \cdots f_k^l)$, $T_k = \begin{pmatrix} T_k^0 & \cdots & 0 \\ \vdots & & \vdots \\ 0 & \cdots & T_k^u \end{pmatrix}$, $g_k = \begin{pmatrix} g_k^0 \\ \vdots \\ g_k^l \end{pmatrix}$, their entries are

$$f_k^l(z_i, z_L) = \mathrm{e}^{\mathrm{i}k(\bar{z}_i - \bar{z}_L)\cdot\hat{s}(\beta_l)}, \tag{15}$$

$$g_k^l(z_c, z) = \mathrm{e}^{\mathrm{i}k(\bar{z} - \bar{z}_c)\cdot\hat{s}(\beta_l)}, \tag{16}$$

$$T_k^u(z_L, z_c) = \sum_{m=-M}^{M} \mathrm{i}^{-m} H_m^1(u)\mathrm{e}^{\mathrm{i}m(\theta_{\bar{u}} - \beta_l)}, \tag{17}$$

where $l = 0, 1, \cdots, L-1$ and $\beta_l = \frac{2\pi l}{L}$. f_k is related to moment, and g_k is the local expansion coefficient, matrix T_k is the transfer function which converts the far enough element moments to local expansion.

Integer L and M in (14) and (17) are the truncation number of Graf addition formula and trapezoidal point number of numerical integral of Bessel integral identity. The integer L and M, which vary from level to level, are crucial to the memory size, accuracy, efficiency and stability of diagonal form FMBEM. An intuitive explanation of the source of numerical error and remarks on truncation number selection were provided[15]. Error analysis of diagonal form expansion and automatic truncation number selection of M for 2D acoustic problems were described in detail in [9, 27]. The "natural selection" of $L = 2M + 1$ was used in [9–10], which can make the transfer matrix evaluation fast by using discrete fast Fourier transfer. We gave an error analysis of numerical integral of Bessel integral identity with the "natural selection"[28]. A semi-empirical formula for truncation length, which is written as $M = y + 5\log(y + \pi)$, where y is the max cluster's radius at one level multiplying wave number[29].

4 The fast multipole method-formulation

We review the formulations for M, M2M, M2L, and L2L in this section. Consider the following integral with kernel H_0^1 in (6):

$$\mathcal{L}_{ij} = \int_{\Gamma_j} G(\bar{z}, \bar{z}_i) q_j(z) \mathrm{d}\tau(z), \tag{18}$$

in which Γ_j is the discrete segment of boundary Γ and away from field point z_i (see Fig. 2).

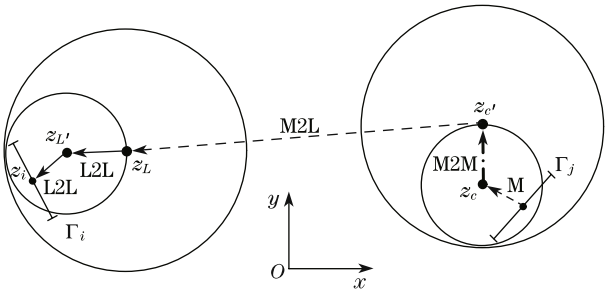

Fig. 2 Geometry of FMBEM building blocks: M, M2M, M2L, and L2L

4.1 Moments (M)

Substituting (14) into (18), we obtain

$$\mathcal{L}_{ij} \approx \frac{\mathrm{i}}{4L}\int_{\Gamma_j} f_k(z_i, z_{L'})T_k(z_{L'}, z_c)g_k(z_c, z)q_j(z)\mathrm{d}\tau(z)$$

$$= \frac{\mathrm{i}}{4L} f_k(z_i, z_{L'})T_k(z_{L'}, z_c)M_k(z_c), \tag{19}$$

where

$$M_k(z_c) = \int_{\Gamma_j} g_k(z_c, z)q_j(z)\mathrm{d}\tau(z) \tag{20}$$

are called moments about z_c, which are independent of the field point z_i and only need to be computed once. And the entry of vector $M_k(z_c)$ is

$$M_k^l(z_c) = \int_{\Gamma_j} \mathrm{e}^{-\mathrm{i}k(\bar{z}-\bar{z}_c)\cdot\hat{s}(\beta_l)}q_j(z)\mathrm{d}\tau(z). \tag{21}$$

After these moments are evaluated, the integral $\mathcal{L}_{ij}$ can be calculated readily using (19) for any field point z_i away from segment Γ_j. in which field point z_i and segment Γ_j should be separated by a pair of separate clusters centered at z_L and z_c, respectively.

4.2 Moment-to-moment translation (M2M)

If the point z_c is moved to a new location $z_{c'}$ (see Fig. 2), the following translation holds for the moment

$$M_k^l(z_{c'}) = \mathrm{e}^{-\mathrm{i}k(\bar{z}_{c'}-\bar{z}_c)\cdot\hat{s}(\beta_l)}M_k^l(z_c) \tag{22}$$

so that

$$\mathcal{L}_{ij} \approx \frac{\mathrm{i}}{4L} f_k(z_i, z_{L'})T_k(z_{L'}, z_c)M_k(z_c) \approx \frac{\mathrm{i}}{4L} f_k(z_i, z_{L'})T_k(z_{L'}, z_{c'})M_k(z_{c'}). \tag{23}$$

And the moments about $z_{c'}$ can be written as

$$M_k(z_{c'}) = B(z_{c'}, z_c)M_k(z_c), \tag{24}$$

where $B(z_{c'}, z_c)$ is a diagonal matrix with entry $B_k^l(z_{c'}) = \mathrm{e}^{-\mathrm{i}k(\bar{z}_{c'}-\bar{z}_c)\cdot\hat{s}(\beta_l)}$, which is called M2M translation for moments when z_c is moved to $z_{c'}$. Note that a new cluster centered at $z_{c'}$ should contain segment Γ_j and be away from that cluster containing the field point z_i. This ensures the existence of (24).

4.3 Moment-to-local translation (M2L)

Incorporate the matrix-vector at the right hand side of (23) and rewrite it as

$$\mathcal{L}_{ij} \approx \frac{\mathrm{i}}{4L} f_k(z_i, z_{L'})L_k(z_L), \tag{25}$$

where

$$L_k(z_L) = T_k(z_{L'}, z_{c'})M_k(z_{c'}) \tag{26}$$

is defined as M2L translation. M2L translation translates the source points contribution from the source cluster to the field cluster.

4.4 Local-to-local expansion (L2L)

Supposing $z_{L'}$ is another cluster's centroid and also locating in the cluster centered at z_L, the following translation holds for f_k

$$f_k^l(z_i, z_L) = f_k^l(z_i, z_{L'})\mathrm{e}^{-\mathrm{i}k(\bar{z}_{L'}-\bar{z}_L)\cdot\hat{s}(\beta_l)}. \tag{27}$$

We have

$$\mathcal{L}_{ij} \approx \frac{\mathrm{i}}{4L} f_k(z_i, z_L) L_k(z_L) = \frac{\mathrm{i}}{4L} f_k(z_i, z_{L'}) L_k(z_{L'}) \tag{28}$$

and

$$L_k(z_{L'}) = D_k(z_{L'}, z_L) L_k(z_L), \tag{29}$$

where $D_k(z_{L'}, z_L)$ is also a diagonal matrix with entry $D_k^l(z_{L'}, z_L) = \mathrm{e}^{\mathrm{i}k(\bar{z}_{L'}-\bar{z}_L)\cdot\hat{s}(\beta_l)}$, which is called L2L translation for local expansion when z_L is moved to a new center $z_{L'}$.

4.5 Expansion for integrals with derivative kernel

Consider the following derivative kernel in (6):

$$\mathcal{M}_{ij} = \int_{\Gamma_j} \frac{\partial G(\bar{z}, \bar{z}_i)}{\partial n(z)} q_j(z) \mathrm{d}\tau(z), \tag{30}$$

$$\mathcal{M}_{ij}^T = \int_{\Gamma_j} \frac{\partial G(\bar{z}, \bar{z}_i)}{\partial n(z_i)} q_j(z) \mathrm{d}\tau(z), \tag{31}$$

$$\mathcal{N}_{ij} = \int_{\Gamma_j} \frac{\partial^2 G(\bar{z}, \bar{z}_i)}{\partial n(z_i) \partial n(z)} \varphi_j(z) \mathrm{d}\tau(z), \tag{32}$$

in which Γ_j is also the discrete segment of boundary Γ and away from field point z_i (see Fig. 2).

Substituting (14) into (30)–(32), we have

$$\mathcal{M}_{ij} \approx \frac{\mathrm{i}}{4L} \int_{\Gamma_j} f_k(z_i, z_{L'}) T_k(z_{L'}, z_c) \frac{\partial}{\partial n(z)} \big(g_k(z_c, z) q_j(z)\big) \mathrm{d}\tau(z), \tag{33}$$

$$\mathcal{M}_{ij}^T \approx \frac{\mathrm{i}}{4L} \int_{\Gamma_j} \frac{\partial f_k(z_i, z_{L'})}{\partial n(z_i)} T_k(z_{L'}, z_c) g_k(z_c, z) q_j(z) \mathrm{d}\tau(z), \tag{34}$$

$$\mathcal{N}_{ij} \approx \frac{\mathrm{i}}{4L} \int_{\Gamma_j} \frac{\partial f_k(z_i, z_{L'})}{\partial n(z_i)} T_k(z_{L'}, z_c) \frac{\partial}{\partial n(z)} g_k(z_c, z) \varphi_j(z) \mathrm{d}\tau(z). \tag{35}$$

The derivative of g_k and f_k are easy to compute, the corresponding entries of their derivative are

$$\frac{\partial}{\partial n(z)} g_k^l(z_c, z) = -\mathrm{i}k\hat{n}(z) \cdot \hat{S}(\beta_l) g_k^l(z_c, z), \tag{36}$$

$$\frac{\partial}{\partial n(z_i)} f_k^l(z_c, z) = \mathrm{i}k\hat{n}(z_i) \cdot \hat{S}(\beta_l) f_k^l(z_c, z), \tag{37}$$

where $\hat{n}(*)$ is the unit normal vector at fixed point "$*$". Therefore moment of integral $\mathcal{M}_{ij}^T$ is the same as the one of $\mathcal{L}_{ij}$. $\mathcal{M}_{ij}^T$ and $\mathcal{N}_{ij}$ have the same moment,

$$M_k^l(z_c) = -\mathrm{i}k \int_{\Gamma_j} \hat{n}(z) \cdot \hat{S}(\beta_l) \mathrm{e}^{-\mathrm{i}k(\bar{z}-\bar{z}_c)\cdot\hat{S}(\beta_l)} \varphi_j(z) \mathrm{d}\tau(z). \tag{38}$$

It can be shown that the M2M, M2L, and L2L translations remain the same for the four integrals, except for the fact that moments of $\mathcal{M}_{ij}$ and $\mathcal{N}_{ij}$ should be calculated by (38) and the final evaluation of $\mathcal{M}_{ij}^T$ and $\mathcal{N}_{ij}$ should be scaled by $\mathrm{i}k\hat{n}(z_i) \cdot \hat{S}(\beta_l)$.

5 Programming for FMBEM

In this section, we first describe a data structure for constructing the quad tree which can simplify the implementation of the FMBEM. An analytical moment is then proposed. And some remarks on technique problem in programming implementation are discussed at the end.

5.1 Data structure

Firstly, we show how to divide a square by quad tree structure. As shown in Fig. 3, the minimum square which covers the entire boundary is the root of the quad tree and is called as the cell of level 0. Divide the square into 4 child cells of level 1 whose length is half of that of the parent cell and number them from left bottom to right top as 0, 1, 2, 3. Continue dividing in this way, i.e., dividing all the cells in level L into 4 equal child cells will generate $2^{2(L+1)}$ cells of level $L+1$ and number them as 0, 1, $\cdots$, $2^{2(L+1)}-1$. Stop dividing until certain condition is reached. A cell having no child cells is called a leaf.

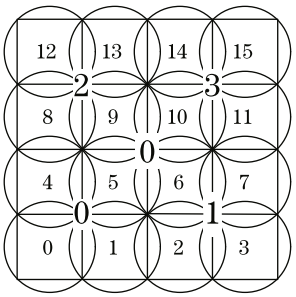

Fig. 3 Quad tree discretization

After discretization, a quad tree which enables search from leaf to root and also from root to leaf can be constructed by the cell number. Define a nonnegative integer a divided by a nature number b as $a/b = [a/b] + (a/b)$, where $[a/b]$ is the quotient and (a/b) is the remainder. For a cell numbered as m at level L, its parent cell number p_m at level $L-1$ is defined as

$$p_m = [[m/2^L]/2] \cdot 2^{L-1} + [(m/2^L)/2]. \tag{39}$$

While the start number c_m^{s} and end number c_m^{e} of its child at level $L-1$ are defined as

$$c_m^{\mathrm{s}} = [m/2^L] \cdot 2^{L+2} + (m/2^L) \cdot 2, \tag{40}$$

$$c_m^{\mathrm{e}} = [m/2^L] \cdot 2^{L+2} + 2^{L+1} + (m/2^L) \cdot 2 + 1. \tag{41}$$

Thus, the quad tree structure can be described by an array in the computer, as shown in Fig. 4.

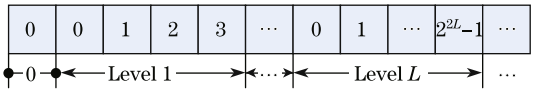

Fig. 4 Array-data structure for quad tree

5.2 Analytical moment

To calculate the moment on the element which in essential is the line integration, several numerical methods are ready to use, such as Gauss integral. While we find the moment calculation for constant element can be done analytically which can somewhat improve the performance of diagonal FMBEM. Since the unit direction $\hat{n}(z)$ of a constant element is also a constant, we just need to derive the expression of the moment for $\mathcal{L}_{ij}$ and $\mathcal{M}_{ij}^T$, moment of $\mathcal{M}_{ij}$ and $\mathcal{N}_{ij}$ is similar to that of $\mathcal{L}_{ij}$ and $\mathcal{M}_{ij}^T$ with difference by a factor $-\mathrm{i}k\hat{n}(z)\cdot\hat{S}(\beta_l)$ and replacement of $q(z)$ with $\varphi(z)$.

To get the analytical moment, firstly, we need to define a way in which we can pass from the global Cartesian coordinates to the local coordinates defined over the element. Suppose two end nodes of element j are $\bar{z}_j$ and $\bar{z}_{j+1}$. By using local coordinates, the coordinates of point $\bar{z}=[x\ y]$ on element j can be expressed as

$$\bar{z}=[x_{j+1}-x_j \quad y_{j+1}-y_j]\xi+[x_j\ y_j]=\overline{N}\xi+\bar{z}_j, \tag{42}$$

where $\overline{N}$ are 2D vectors defined by (42), $\xi=\|\bar{z}-\bar{z}_j\|/L_j$, and L_j is defined by $L_j=\|\bar{z}_{j+1}-\bar{z}_j\|$.

Substituting (42) into (21), we have

$$M_k^l(z_c)=L_jq_j\mathrm{e}^{\mathrm{i}k(\bar{z}_c-\bar{z}_j)\cdot\hat{S}(\beta_l)}\int_0^1\mathrm{e}^{-\mathrm{i}k\overline{N}\cdot\hat{S}(\beta_l)\xi}\mathrm{d}\xi. \tag{43}$$

If $\overline{N}\cdot\hat{S}(\beta_l)$ is not equal to zero, which means the vector $\overline{N}$ is not perpendicular to vector $\hat{S}(\beta_l)$, we have

$$M_k^l(z_c)=\frac{L_jq_j}{\mathrm{i}k\overline{N}\cdot\hat{S}(\beta_l)}(1-\mathrm{e}^{-\mathrm{i}k\overline{N}\cdot\hat{S}(\beta_l)})\mathrm{e}^{\mathrm{i}k(\bar{z}_c-\bar{z}_1)\cdot\hat{S}(\beta_l)}. \tag{44}$$

If $\overline{N}\cdot\hat{S}(\beta_l)$ is equal to zero, we have

$$M_k^l(z_c)=L_jq_j\mathrm{e}^{\mathrm{i}k(\bar{z}_c-\bar{z}_j)\cdot\hat{S}(\beta_l)}. \tag{45}$$

The analytical moment derivation is direct without loss of accuracy. It is no doubt that computing moment by the analytical way is more accurate, stable and efficient than numerical integral method. Although analytical moment derived here is for constant element, the analytical moment for linear element is ready to get.

5.3 Interpolation

Because the trapezoidal point number L depends on the quad tree cell size, it increases at upward pass and decreases at downward pass. Interpolation is needed to compute moment at lower levels from calculated moment at higher levels, and to compute local expansion in the inverse way of moment computation. It is easy to get from (21) that the moment of diagonal

FMBEM is actually a function of angle β in the range from 0 to 2π. By using Jacobi-Anger expansion, moments can be written as

$$M_k(z_c) = \sum_{n=-\infty}^{\infty} a_n \mathrm{e}^{\mathrm{i}n\beta}, \tag{46}$$

where $a_n = \int_{\triangle\Gamma} \mathrm{i}^n J_n(k\|\bar{z} - \bar{z}_c\|)\mathrm{e}^{\mathrm{i}n\beta}\mathrm{d}\tau(z)$. Since $|J_{|n|}(x)|$ is a strictly decreasing function with respect to $|n|$ for fixed x. If $|n| > x$, $|J_{|n|}(x)| \cong 0$ when $|n| > N$ supposing N is a large enough truncation number. That means moments can be treated as band limited function with acceptable error. To get the coefficient $a_n(|n| \leqslant N)$, we perform Fourier transform with respect to the computed moments. Once all the coefficient $a_n(|n| \leqslant N)$ are calculated, moments at any other point β' can be easily calculated using (46) for $|n| \leqslant N$. That is the idea of uniform resolution interpolation[30] and also the method we used in this paper. Since the transform function is a band limited function of angle β and local expansion is the product of moment and transform function, uniform resolution interpolation is also used in downward process.

5.4 Preconditioning and storing coefficients

Sharp corners, high frequency and so on may cause ill conditions of the linear systems appearing in the BEM. Therefore, preconditioning is necessary to the solution using an iterative solver (GMRES). In this paper, we adopt block diagonal preconditioning which uses a list of elements contained inside childless cell in the quad tree. Since the preconditioning matrix is sparse, we calculate the preconditioning matrix once and store it for all iterations in the solution of FMBEM. This also provides an option to reuse the coefficients in the direct evaluation of downward process[12–14].

6 Numerical examples

The algorithm is implemented in Fortran 90 and tested on a computer with an Intel Dual Core 2.2 GHz CPU, 2 GB RAM. Constant triangular elements are used in our study, for which one can evaluate the singular integrals analytically. The GMRES solver is applied to solve the FMBEM and the tolerance is set to 10^{-4}.

6.1 Scattering from rigid cylinder

As an example to test the accuracy of the program, we compute acoustic wave scattered by an infinite rigid cylinder of radius a with a plane incident wave of unit amplitude travelling along the positive x axis ($\theta = 0$) in a direction perpendicular to the axis of the cylinder. The characteristic length (CL), defined by wave number multiplying side length of minimum square containing the model, of infinite cylinder is equal to 5. Sample filed points are evenly distributed on a circle of $r = 2a$, as shown in Fig. 5. Exact field pressure at point (r, θ) is given as[31]

$$\varphi(r,\theta) = -\sum_{m=0}^{\infty} \varepsilon_m \mathrm{i}^m \frac{\mathrm{J}_{m'}(ka)}{H^1_{m'}(ka)} H^1_m(kr)\cos(m\theta), \tag{47}$$

where ε_m is Neumann constant, "$'$" means derivative with respect to ka, J_m is the mth Bessel function of the first kind. The field pressure plotted in Fig. 6 shows that the accuracy of the program.

Since acoustic scattering problems are frequency dependent, to further demonstrate that the program is accurate for a wide range of frequencies, another example for the rigid cylinder scattering with varying frequencies is performed. The CL of the model is increasing from 6 to 60, the corresponding boundary element numbers used in the simulation are listed in

Table 1. Boundary solutions given by FMBEM and analytical way are compared. Relative errors listed in Table 1 are defined in L2 sense with respect to analytical solutions. In Table 1, DOF means boundary element number, Trel means the lowest tree level, Iter means the number of iterations, RPD and NPD means solution with right preconditioning and no preconditioning respectively.

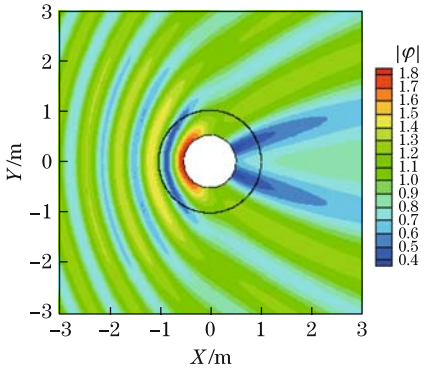

Fig. 5 Field pressure contour plot for scattering of rigid cylinder

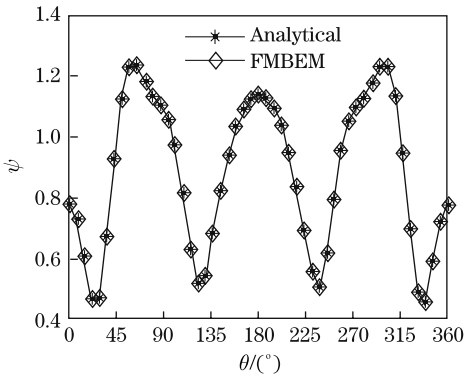

Fig. 6 Field pressure given by analytical and FMBEM

Table 1 Results of rigid cylinder scattering with varying frequency

CL	DOF	Trel	Iter		Relative error
			RPD	NPD	
6	4 000	4	6	15	2.593 0E–4
12	12 700	6	9	21	5.439 3E–4
18	22 400	6	12	24	1.692 7E–4
24	32 100	6	16	31	6.916 5E–4
30	51 500	7	21	41	7.856 9E–4
36	61 200	7	24	44	2.799 6E–4
42	70 900	7	27	55	3.092 2E–4
48	80 600	7	28	57	1.683 3E–4
54	90 300	7	30	70	3.070 8E–4
60	100 000	8	34	79	1.651 3E–4

6.2 Scattering from multi-cylinders

FMBEM with right preconditioning is applied to compute the acoustic scattering by multi-cylinders with a plane incident wave of unit amplitude travelling along the positive x axis ($\theta = 0$) as shown in Fig. 7. The multiple scattering model contains 300 random located cylinders in a square. The field is meshed with 29 004 2D triangular elements. The characteristic length of this model is 40. Maximum element allowed in a leaf is set to be 70. The boundary and filed pressure solutions are all computed by the FMBEM. Analytical field solution of this model is not available. Theoretically, increasing the element number in the boundary discretization will make the field solution converge to the exact solution. Field solution with boundary discretized with 210 000 elements is plotted in Fig. 7, and taken as a benchmark solution to explore the accuracy of the program in the complex model solution. Relative errors with respect to the benchmark solution in L2 sense are evaluated and plotted in Fig. 8. Obviously, Figure 8 demonstrates the convergence of refining the boundary mesh, and implicates the accuracy of

the algorithm. The CPU time used in boundary solution (FMBEM) and filed pressure evaluation (FMFE) by the fast multipole method, as well as the field pressure evaluation by direct method (DFE) are plotted in Fig. 9, which shows the computing efficiency of the FMBEM for large scale acoustic problems solution.

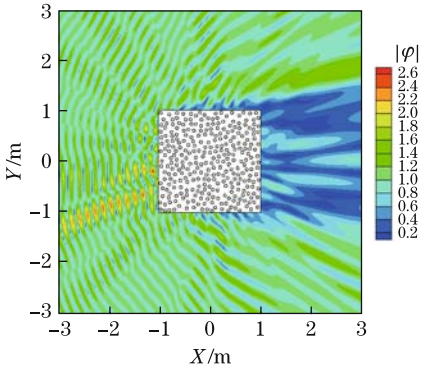

Fig. 7 Field pressure contour plot of multi-cylinders scattering

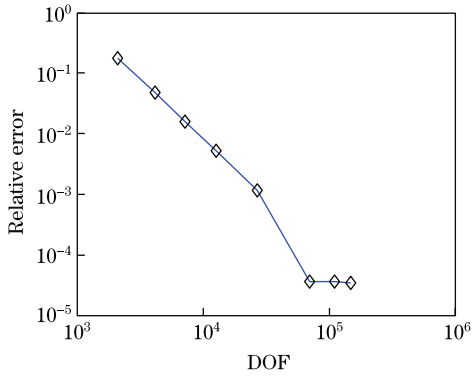

Fig. 8 Relative errors of different discretization with respect to benchmark solution

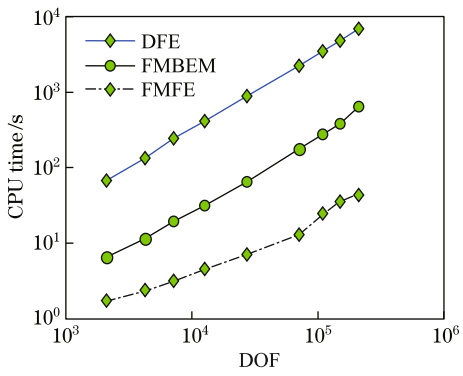

Fig. 9 CPU time used in boundary solution and filed evaluation of different discretization

6.3 Radiation of vibrating rail

Railway is entering an era of higher speed. The noise generated by rails due to the impact of wheels and rails is significant at high speed. The sound radiation from a vibrating rail can be predicted using a two-dimensional model under certain conditions: (i) The structural wavelength in the rail is much longer than the wavelength of sound in air at the same frequency, and (ii) the decay of vibration with distance along the rail is small. If condition (ii) is not satisfied, two-dimension rail mode is still appropriate if the boundary value is selected at the force point. To simplify that, we simulate the sound radiation of harmonic respond. The boundary value generated by harmonic force applied on the top line of rail model is firstly computed by a third party CAE program. Then we use the FMBEM to simulate the sound radiation of the vibrating rail based pm the computed boundary value as shown in Fig. 10. The characteristic length of rail model is 25. The rail is meshed with 22 956 line elements and its field is meshed with 32 817 triangular elements. The total time used for boundary solution and field evaluation is 88.83s. The simulation results are summarized in Table 2.

Table 2 Results of simulation

Case	Rail radiation	Case		Rail radiation	Case	Rail radiation
CL	25	RPD	Iter	55	Field DOF	32 817
			CPU time	42.62	Field Trel	7
DOF	22 956	NPD	Iter	122	FMFE CPU time	46.21
Model Trel	6		CPU time	92.87	DFE CPU time	1 962.26

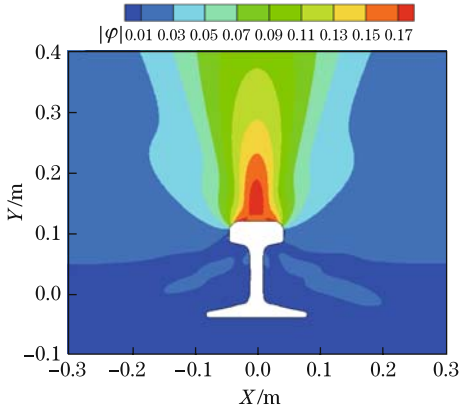

Fig. 10 Radiation of vibration rail

7 Discussion

This paper presents the FMBEM for 2D acoustic wave problems. The kernel function expansion theory is summarized. An analytical expression for moment computation is derived which is more accurate, stable, and efficient. A data structure is proposed which can simplify the quad-tree construction. Formulations and implementation details are also provided which can help readers to understand the 2D acoustic FMBEM.

Numerical examples of acoustic scattering by an infinite cylinder with a hard surface incidenced by a plane wave are investigated to demonstrate the accuracy. The applications of FMBEM in solving multi-cylinder scattering and simulating the vibrating rail radiation further demonstrate the efficiency as well as the accuracy of the FMBEM. Since the larger the CL or the more complicated the model, the more ill-conditioned the corresponding linear equations is, preconditioning is very important in the iteration solution. We used right block diagonal preconditioning in this paper. Results listed in tables show that preconditioning can make great improvement compared with solution without preconditioning. Although preconditioning reduces the iteration number for large CL and complicated model, the time used for one iteration is more than that of solution without preconditioning because preconditioning will take extra time for matrix inverse process.

Since diagonal FMBEM is not stable for small CL, for fixed CL the element number allowed in a leaf should increase with respect to the element number of the model. The memory used for storing direct coefficients and time for preconditioning will also increase. A method combined the adaptive FMBEM and wideband FMBEM which is suitable for a wide range CL is under development.

References

[1] Copley, L. G. Integral equation method for radiation from vibrating bodies. *Journal of the Acoustical Society of America*, **41**(4A), 807–816 (1967)

[2] Schenck, H. A. Improved integral formulation for acoustic radiation problems. *Journal of the Acoustical Society of America*, **44**(1), 41–48 (1968)

[3] Meyer, W. L., Bell, W. A., Zinn, B. T., and Stallybrass, M. P. Boundary integral solutions of three dimensional acoustic radiation problems. *Journal of Sound and Vibration*, **59**(2), 245–262 (1978)

[4] Terai, T. On calculation of sound fields around three dimensional objects by integral equation methods. *Journal of Sound and Vibration*, **69**(1), 71–100 (1980)

[5] Rokhlin, V. Rapid solution of integral equations of classical potential theory. *Journal of Computational Physics*, **60**(2), 187–207 (1985)

[6] Greengard, L. and Rokhlin, V. A fast algorithm for particle simulations. *Journal of Computational Physics*, **73**(2), 325–348 (1987)

[7] Greengard, L. *The Rapid Evaluation of Potential Fields in Particle Systems*, MIT Press, Cambridge (1988)

[8] Rokhlin, V. Rapid solution of integral equations of scattering theory in two dimensions. *Journal of Computational Physics*, **86**(2), 414–439 (1990)

[9] Amini, S. and Profit, A. T. J. Analysis of a diagonal form of the fast multipole algorithm for scattering theory. *BIT Numerical Mathematics*, **39**(4), 585–602 (1999)

[10] Amini, S. and Profit, A. T. J. Multi-level fast multipole solution of the scattering problem. *Engineering Analysis with Boundary Elements*, **27**(5), 547–564 (2003)

[11] Chen, J. T. and Chen, K. H. Applications of the dual integral formulation in conjunction with fast multipole method in large-scale problems for 2D exterior acoustics. *Engineering Analysis with Boundary Elements*, **28**(6), 685–709 (2004)

[12] Shen, L. and Liu, Y. J. An adaptive fast multipole boundary element method for three-dimensional acoustic wave problems based on the Burton-Miller formulation. *Computational Mechanics*, **40**(3), 461–472 (2007)

[13] Bapat, M. S., Shen, L., and Liu, Y. J. Adaptive fast multipole boundary element method for three-dimensional half-space acoustic wave problems. *Engineering Analysis with Boundary Elements*, **33**(8-9), 1113–1123 (2009)

[14] Liu, Y. J. *Fast Multipole Boundary Element Method*: *Theory and Applications in Engineering*, Cambridge University Press, Cambridge (2009)

[15] Crutchfield, W., Gimbutas, Z., Greengard, L., Huang, J., Rokhlin, V., Yarvin, N., and Zhao, J. Remarks on the implementation of wideband FMM for the Helmholtz equation in two dimensions. *Contemporary Mathematics*, **408**, 99–110 (2006)

[16] Cheng, H., Crutchfield, W. Y., Gimbutas, Z., Greengard, L. F., Ethridge, J. F., Huang, J., Rokhlin, V., Yarvin, N., and Zhao, J. A wideband fast multipole method for the Helmholtz equation in three dimensions. *Journal of Computational Physics*, **216**(1), 300–325 (2006)

[17] Gumerov, N. A. and Duraiswami, R. A broadband fast multipole accelerated boundary element method for the three dimensional Helmholtz equation. *Journal of the Acoustical Society of America*, **125**(1), 191–205 (2009)

[18] Liu, Y. J. and Nishimura, N. The fast multipole boundary element method for potential problems: a tutorial. *Engineering Analysis with Boundary Elements*, **30**(5), 371–381 (2006)

[19] Ciskowski, R. D. and Brebbia, C. A. *Boundary Element Methods in Acoustics*, 1st ed., Springer, New York (1991)

[20] Burton, A. J. and Miller, G. F. The application of integral equation methods to the numerical solution of some exterior boundary-value problems. *Proceedings of the Royal Society of London, Series A, Mathematical and Physical Sciences*, **323**(1553), 201–210 (1971)

[21] Kress, R. Minimizing the condition number of boundary integral operators in acoustic and electromagnetic scattering. *Quarterly Journal of Mechanics and Applied Mathematics*, **38**(2), 323–341 (1985)

[22] Colton, D. and Kress, R. *Integral Equation Methods in Scattering Theory*, Wiley, New York (1983)

[23] Abramowitz, M. and Stegun, I. A. *Handbook of Mathematical Functions with Formulas, Graphs, and Mathematical Tables*, U.S. Govt. Print. Off., Washington (1964)

[24] Saad, Y. and Schultz, M. H. GMRES: a generalized minimal residual algorithm for solving non-symmetric linear systems. *SIAM Journal on Scientific and Statistical Computing*, **7**(3), 856–869 (1986)

[25] Sonneveld, P. GGS: a fast Lanczos-type solver for nonsymmetric linear systems. *SIAM Journal on Scientific and Statistical Computing*, **10**, 36–52 (1989)

[26] Labreuche, C. A convergence theorem for the fast multipole method for 2 dimensional scattering problems. *Mathematics of Computation*, **67**(222), 553–591 (1998)

[27] Amini, S. and Profit, A. Analysis of the truncation errors in the fast multipole method for scattering problems. *Journal of Computational and Applied Mathematics*, **115**(1-2), 23–33 (2000)

[28] Wu, H. J., Jiang, W. K., and Liu, Y. J. Analysis of numerical integration error for Bessel integral identity in fast multipole method for 2D Helmholtz equation. *Journal of Shanghai Jiaotong University* (*Science*), **15**(6), 690–693 (2010)

[29] Coifman, R., Rokhlin, V., and Wandzura, S. The fast multipole method for the wave equation: a pedestrian prescription. *Antennas and Propagation Magazine*, *IEEE*, **35**(3), 7–12 (1993)

[30] Jakob-Chien, R. and Alpert, B. K. A fast spherical filter with uniform resolution. *Journal of Computational Physics*, **136**(2), 580–584 (1997)

[31] Morse, P. M. and Ingard, K. U. *Theoretical Acoustics*, Princeton University Press, Princeton, New Jersey (1987)